Chapter 17
Global Mercury Modelling at Environment Canada

Ashu P. Dastoor and Didier Davignon

Summary We describe the recent developments of Environment Canada's atmospheric mercury model (GRAHM) and its application to the intercontinental source-receptor relationships of mercury. The model includes 2188 Mg yr^{-1} global anthropogenic emissions, 1600 Mg yr^{-1} terrestrial emissions and 2600 Mg yr^{-1} oceanic emissions). Transport, chemical transformation and deposition of Hg^0, $Hg^{(II)}$ and Hg(p) are simulated in GRAHM within a meteorological assimilation and forecasting system. Current version of the GRAHM includes GEM oxidation by ozone in the troposphere and halogen oxidation in the Polar and the marine boundary layers. It also includes dynamic exchange of mercury fluxes at air-snow/ice interface. The model simulates springtime atmospheric mercury depletion events (AMDEs) and the net accumulation of mercury in snow in the Polar Regions. We performed one reference simulation with emissions as above and four perturbation simulations with 20% reduced anthropogenic emissions over East Asia, South Asia, Europe and North Africa and North America. 20% reduction in anthropogenic emissions of mercury over East Asia, South Asia, Europe and North Africa and North America represent 7.7%, 1.6%, 2.5% and 1.3% reduction in global anthropogenic emissions respectively. The deposition over East Asia, South Asia, Europe and North America are reduced by 13.5%, 7.9%, 8.3% and 4.3% due to the emission reductions within the same regions. Deposition in North America is found to be most affected by the emission reductions in other regions and the deposition in East Asia is least affected by outside reductions. The deposition in the Arctic is nearly equally sensitive to the unit emission reductions in Europe and East Asia and is most sensitive in springtime due to the high deposition related to AMDEs.

17.1 Introduction

Hg is on the priority list of a large number of international agreements, conventions and national advisories aimed at the protection of the environment including all compartments, human health and wildlife (e.g. CLRTAP, AMAP, UN-ECE, HELCOM, OSPAR and many more). The mercury methylation process is shown to be strongly correlated with loadings of inorganic mercury to the aquatic system

N. Pirrone and R. Mason (eds.), *Mercury Fate and Transport in the Global Atmosphere*,
DOI: 10.1007/978-0-387-93958-2_17,

from the atmosphere (Hammerschmidt et al., 2004). Ambient measurements of mercury reveal a vast global pool of mercury in the atmosphere up to the tropopause revealing its global nature and yet at the same time, atmospheric measurements of mercury in polar regions, in marine boundary layer and in the upper troposphere have shown that elemental mercury can be rapidly oxidized to more hygroscopic forms and deposited at much shorter time scales. In the atmosphere, mercury is mainly present as gaseous elemental mercury (GEM), reactive gaseous mercury (RGM) and particulate mercury (Hg(p)). GEM is the most dominant form of mercury in the atmosphere with the longest life time (0.5 – 2 yr) and RGM and Hg(p) have a significantly shorter lifetime (few days - week) and are deposited rapidly via dry and wet deposition (Lin et al., 2006). Emissions of mercury from natural as well as anthropogenic sources, multiple time scales of mercury in the atmosphere and photochemically and biologically driven revolatilization of mercury at the surface render understanding of global cycling of mercury a challenging subject. The impact of confounding factors such as climate change and changes in other pollutants in the atmosphere add to the complexity of determining the impact of reducing emissions of mercury on deposition.

In this chapter, we briefly describe the Environment Canada's global mercury model GRAHM and provide results on model simulations to assess the impact of reduced anthropogenic emissions from four main source regions of mercury in Northern Hemisphere.

17.2 Model Description

The Global/Regional Atmospheric Heavy Metals Model (*GRAHM*) is an Eulerian, multi-scale meterological and mercury simulation model which is developed by including atmospheric mercury dynamical, physical and chemical processes on-line into Canadian operational weather forecasting and data assimilation model *GEM* (Global Environmental Multiscale Model). Details of the model GRAHM are described in Dastoor and Larocque (2004), Ariya et al. (2004) and Dastoor et al. (2008). Transport, transformation and surface exchange of three mercury species, namely, gaseous elemental mercury (GEM), gaseous divalent mercury (RGM) and particulate mercury (Hg(p)) are simulated in the model. For this study, the anthropogenic mercury emissions were updated to year 2000 (Pacyna et al., 2006). Terrestrial and oceanic emissions of GEM from direct natural sources and from previously deposited mercury were introduced based on the global mercury budget study by Mason and Sheu (2002). Land based natural emissions were spatially distributed according to the natural enrichment of mercury and re-emissions were distributed according to the distribution of total deposition of mercury for historic years. Oceanic emissions in the model are spatially distributed according to the deposition and primary production distribution. Seasonal and diurnal dependence is added to both land and oceanic emissions as a function of solar irradiance.

Following the discussion in Calvert et al. (2005) and the observational constraints of mercury measurements on global scale, we have included slow oxidation of GEM by O_3 reported in Hall, (1995) as the primary oxidation of GEM in the gas phase. Monthly averaged and diurnally varying concentrations of O_3 are specified from a detailed tropospheric chemistry model MOZART (Horowitz et al., 2003). The oxidation product is equally partitioned between RGM and Hg(p). Oxidation of GEM by O_3, OH and reactive chlorine and reduction of RGM by S(IV) and via photolysis of $Hg(OH)_2$ are part of the aqueous phase redox chemistry in the model. Sorption of aqueous mercury species to elemental carbon aerosols is also included in the model. GEM is dry deposited only over forest regions due to its low solubility and it is modelled using a seasonally dependent constant dry deposition velocity in the range of 0.001-0.03 cm s^{-1}. Dry deposition of RGM is parameterized utilizing the multiple resistance analogy. Dry deposition velocity for Hg(p) is parameterized as a function of particle size and density. Both gaseous and particle dry deposition velocities are functions of micro-meteorological conditions, land-use types, surface wetness, snow/ice and surface roughness characteristics. GRAHM, being an on-line model, has the advantage of using detailed cloud micro-physical parameters which are simulated at each time step by the model cloud parameterization schemes which are used for the formation of wet deposition in the model. Mercury removal through the conversion of hydrometeors to precipitation as well as through below cloud scavenging are included in the model.

At polar sunrise, gaseous elemental mercury (GEM) undergoes an exceptional dynamic exchange in the air and at the snow surface, during which GEM can be rapidly removed from the atmosphere (the so called atmospheric mercury depletion events (AMDEs), as well as re-emitted from the snow within a few hours to days in the Polar Regions. During AMDEs, gaseous elemental mercury is converted to hygroscopic mercury species (reactive gaseous mercury and total particulate mercury). Experimental and theoretical studies demonstrate that reactions of GEM with BrO and Br are the most likely mechanism of AMDEs in the Polar Regions (Steffen et al., 2008). Similar to the Polar Regions, diurnally varying elevated concentrations of RGM are also observed in remote marine boundary layer (MBL) suggesting RGM production photochemically by reactions with halogens liberated from sea-salt particles (Laurier et al., 2003). Halogen oxidation of mercury over oceans and the Polar Regions can potentially alter the life time of GEM in the atmosphere and its intercontinental long-range transport. GRAHM includes GEM oxidation by halogen species in the Polar Regions and the MBL. We have included GEM reactions with BrO, Br_2, Br, Cl_2 and Cl using reaction rate coefficients from Ariya et al. (2004). Reported Hg^0-Br reaction rate coefficients range from 1.1×10^{-12} to 3.6×10^{-13} cm^3 $molecules^{-1}$ s^{-1} (Donohoue et al., 2006). Our choice of Hg^0-Br reaction rate coefficient (Ariya et al., 2004) is based on the best correlation estimates between model simulated AMDEs and observed AMDEs at Alert, Canada for multiple years. We have assumed part of the oxidation product of mercury reactions by halogens as RGM and partly as TPM in the absence of full understanding of the heterogeneous chemistry of mercury. Since the dry deposition velocities of RGM and TPM are

much larger compared to GEM, and both, RGM and TPM, are readily deposited to snow, lack of accuracy in partitioning between RGM and TPM is expected to have small impact on the deposition estimates of mercury to the snow.

Sources and processes responsible for bromine liberation in the Arctic boundary layer are not fully understood. Sea-salt aerosols, sea-salt deposits on snow, new sea-ice surfaces and frost flowers have been suggested as sources. In the absence of a complete understanding of these processes, the model includes GOME (Global Ozone Monitoring Experiment) satellite derived monthly average Br/BrO concentrations into the boundary layer of the model. A strong photo-reduction and evasion of mercury deposited to the snowpacks following AMDEs has been observed to reduce significantly the accumulation of mercury of in snowpacks (Poulain et al. 2004; Kirk et al. 2006). Poulain et al. (2004) also found evidence for re-oxidation of reduced GEM in the high Arctic snowpacks due to the presence of oxidative molecules (organic and halides) in the marine/coastal polar surface snow during springtime. Present knowledge on the Hg (photo) redox chemistry in the snow is very limited for model parameterization. We have included evasion of mercury from the snowpacks as a function of solar radiation reaching the surface including the influence of clouds and surface temperature with an assumption that it occurs near the surface from the newly deposited mercury.

17.3 Results and Discussion

The model resolution for this study was $2^{\circ}\times2^{\circ}$ in the horizontal and 28 levels up to 10 hPa in the vertical with higher resolution in the boundary layer. Model simulations were performed for the years 2001 with an initial spin-up for three years with the above configuration. The model was evaluated against the globally observed data. The mercury budgets in various compartments in the model were found to be well balanced. The model simulated yearly average of surface air GEM concentration is 1.8 ng m^{-3} in Northern Hemisphere and 1.3 ng m^{-3} in Southern Hemisphere which are within the range of measured concentrations. North to South gradient of ambient GEM concentrations over the Atlantic and Pacific oceans simulated by the model and its comparison with the observations is shown in Figure 17.1. It was found to be improved in this version of the model compared to the previous version as a result of the addition of halogen mercury chemistry in the MBL.

Figure 17.2 shows seasonal average surface air GEM concentrations and observed and model simulated time series of GEM at Alert, Canada Highest GEM concentrations above 2.4 ng m^{-3} are found over East Asia. The GEM concentrations are highest in wintertime over Europe and North America. Enhanced Northward transport of mercury from Europe in winter and from East Asia in spring is evident in the seasonal average concentrations. Most dramatic seasonal cycle is simulated over the Arctic. In the springtime when AMDEs are active the GEM concentrations are lowest and recover to the background values in fall.

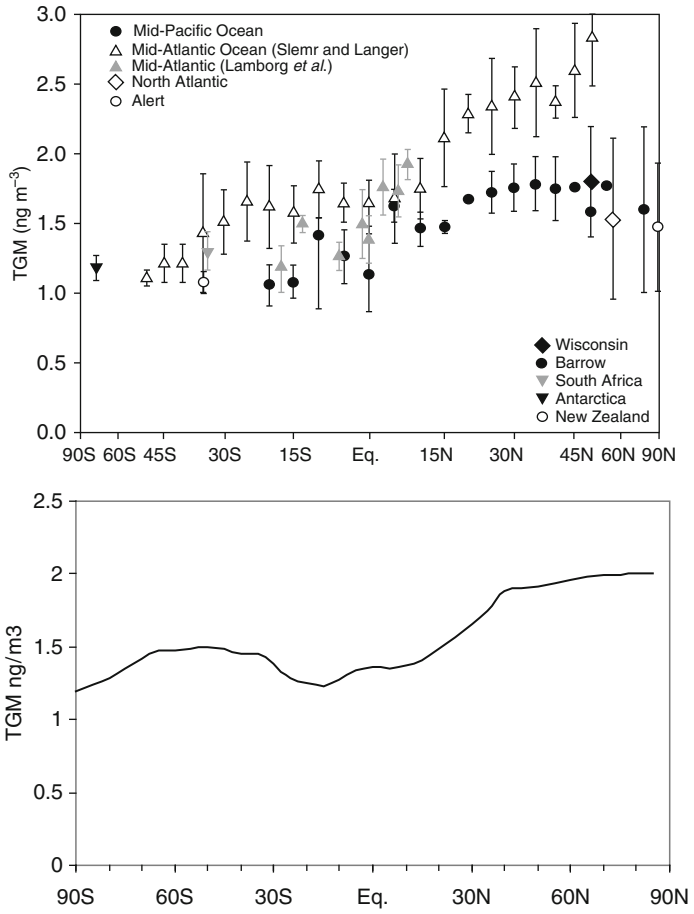

Figure 17.1 Inter-hemispheric gradient of TGM from observations (top) (from Lamborg et al., 2002) and GRAHM model simulation (bottom)

Atmospheric mercury measurements have been conducted in the Arctic at Alert, Barrow, Amderma, Ny-Alesund, and Station Nord (Steffen et al., 2008). Longest record of GEM measurements in the Arctic is available at Alert, Nunavut, which has been continuous since 1995. Rapid exchange of mercury related to AMDEs in springtime is seen in the model simulation and in the observation (Figure 17.1). Strong re-emission events are also observed and simulated in the late spring related to the higher surface temperatures. Br and BrO concentrations used in the model are climatological averages with dependence on the solar influx, boundary layer height and surface temperature. However, despite these limitations, the model captures 1-2 weeks AMDE cycles and the interannual variability in GEM concentrations. These results suggest significant role of meteorological processes such as

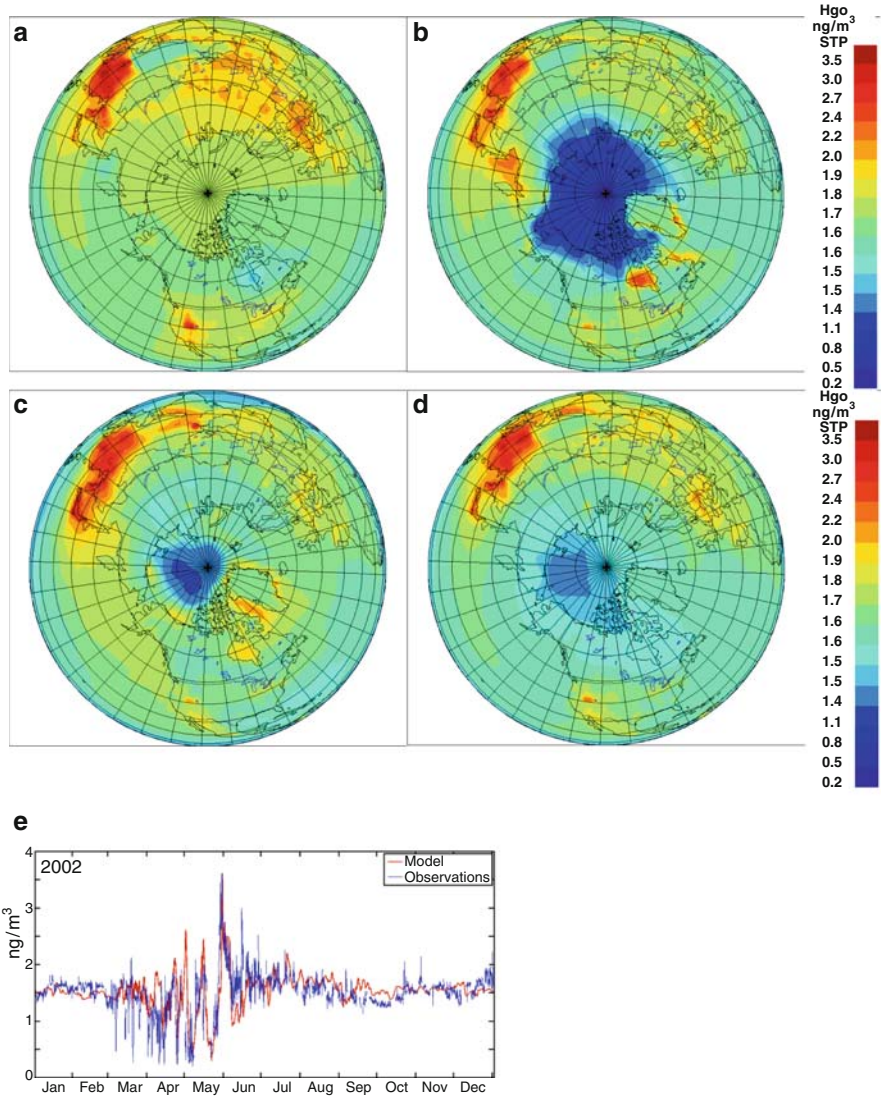

Figure 17.2 GRAHM simulated average surface air Hg^0 concentrations (*ng standard* m^{-3}) for (**a**) winter, (**b**) spring, (**c**) summer and (**d**) fall and (**e**) observed and model simulated time series of surface air Hg^0 concentrations at Alert, Canada for 2002

transport, boundary layer height, solar radiation reaching ground, clouds, temperature inversion and surface temperature in establishing AMDEs. Measured median concentrations of GEM at Alert are 1.61 ng m^{-3} in winter, 1.34 ng m^{-3} in spring, 1.78 ng m^{-3} in summer and 1.53 ng m^{-3} in fall. Model simulated average median surface air concentrations of GEM at Alert are 1.51 ng m^{-3} in winter, 1.35 ng m^{-3} in spring, 1.75 ng m^{-3} in summer and 1.52 ng m^{-3} in fall. Model simulated GEM and RGM air

concentrations at other locations are found to be in the same range as reported in the limited measurements reported in the literature (Steffen et al., 2008).

In addition to the above reference simulation, we conducted four perturbation experiments with 20% reduction in anthropogenic emissions in four major source regions as defined by The Task Force on Hemispheric Transport of Air Pollution. These regions are: East Asia (EA: 15-50N; 95-160E), Europe and North Africa (EU: 25-65N; 10W-50E), South Asia (SA: 5-35N; 50-95E), and North America (NA: 15-55N; 125-60W). Each of these regions represent 841 Mg, 276 Mg, 179 Mg and 143 Mg of total anthropogenic mercury emissions annually respectively. The annual total deposition of mercury from all mercury emissions and the reduction in total deposition of mercury for the four perturbation experiments are illustrated in Figure 17.3.

The wet and dry depositions account for 45% and 55% of total deposition over land and 64% and 36% of total deposition over ocean respectively. Deposition is seen to be high over the mercury source regions and the Polar Regions. The annual total deposition in the four source regions of the perturbation experiments are 593 Mg for East Asia, 232 Mg for Europe and North Africa, 191 Mg for South Asia and 281 Mg for North America.

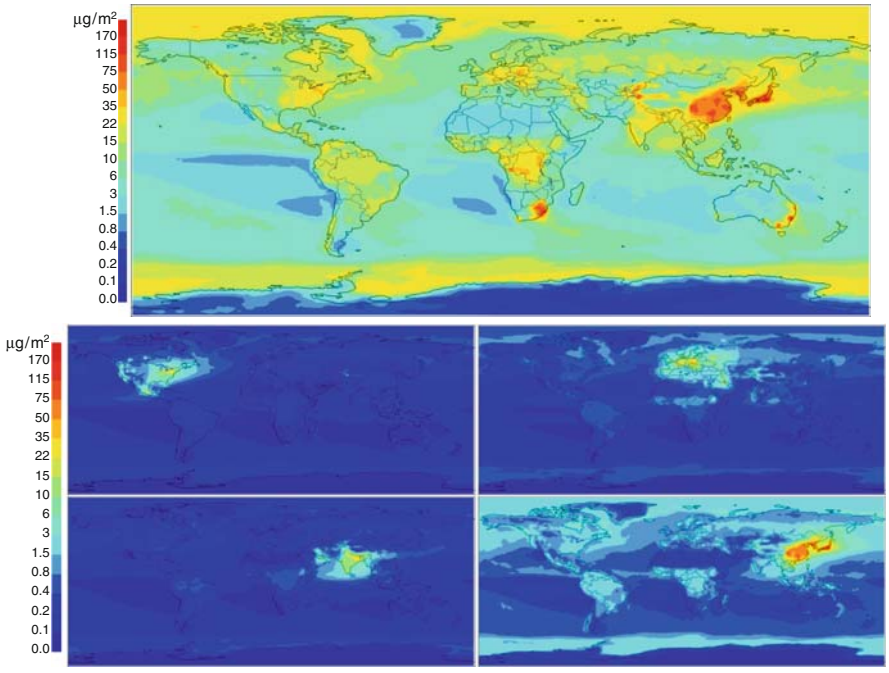

Figure 17.3 Total mercury deposition for year 2001 from reference simulation (top) and reduction in deposition due to 20% reduction in anthropogenic emissions (scaled to 100% in the figure) from North America (middle left), Europe and North Africa (middle right), South Asia (bottom left) and East Asia (bottom right)

The deposition over the Polar Regions is enhanced by the springtime AMDEs. The model estimates deposition of 243 Mg yr^{-1}, and evasion of 145 Mg yr^{-1} resulting in net atmospheric flux of 98 Mg yr^{-1} to the Arctic Ocean (Outridge et al. 2008). The wet deposition simulated by the model is in the range of measured deposition data for North America and Europe. The deposition reduction due to 20% reduction of anthropogenic emissions is seen maximum over the source regions and the regions of high precipitation.

The deposition reductions in the four regions due to reductions in anthropogenic emissions in each of the four regions are summarized in Table 17.1. Wet and dry deposition of mercury mainly occurs as RGM and Hg(p). RGM and Hg(p) emitted in each of the four regions (East Asia: 43%, Europe: 41%, South Asia: 47% and North America: 41%) is mostly deposited regionally due to its short life time of the order of days. Long range transport of elemental mercury to the receptor regions and its oxidation leads to the deposition contribution from intercontinental sources.

Figure 17.4 presents the sensitivities of the surface air GEM concentrations and column GEM burden at receptor regions including the Arctic to unit emissions in each of the four source regions averaged for the four seasons. Surface air is seen to be most sensitive to regional emissions whereas column mercury is most sensitive to the long range transport from East Asia for most regions. The East Asian emissions are located on the eastern seaboard of Asia in the region of mid-latitude cyclones which can facilitate lifting of the pollution to the free troposphere from the boundary layer where it can be transported efficiently.

Surface air in the Arctic region is most sensitive to long range transport in winter from all source regions. The deposition sensitivities to the unit emissions in source regions and the percentage deposition reduction at receptor regions and the Arctic due to emission reductions in each of the four source regions are shown is Figure 17.5. The depositions in all regions are most sensitive to regional emissions. Arctic region is most sensitive to emissions from Europe, East Asia and North America in the springtime.

The AMDEs related high deposition in the Arctic is responsible for high sensitivity during spring. The impact of emission reduction in remote regions to local deposition is maximum for North America where deposition is reduced by 2.8% due to 20% emission reduction in East Asia. Outside impact is minimum for East

Table 17.1 Reduction in mercury deposition (*Mg* yr^{-1}) over four receptor regions and the Arctic due to 20% reduction in emissions from four source regions. First column shows the reduction in emissions for the four source regions

Receptors Sources	Emission reduction	South Africa	East Asia	Europe	North America	Arctic
South Asia	35.7	15.1	2.3	0.7	1.0	0.9
East Asia	168.2	3.6	80.0	4.2	7.1	8.0
Europe	55.1	1.8	1.8	19.2	1.7	2.7
N. America	28.6	0.4	0.8	0.8	12.2	1.2

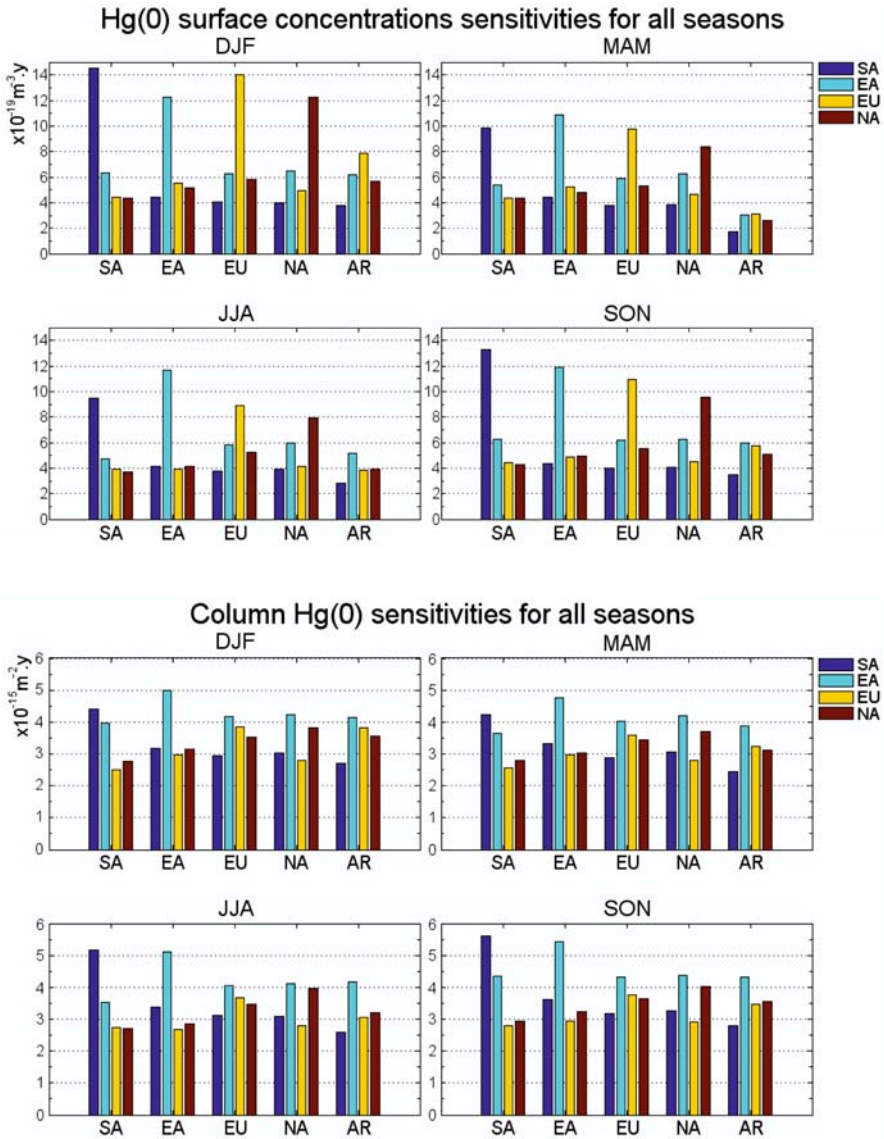

Figure 17.4 The surface air GEM concentration (top) and column GEM burden (bottom) sensitivities at receptor regions (x axis) and the Arctic to unit emission reductions from the source regions defined as South Asia (SA), East Asia (EA), Europe and North Africa (EU) and North America (NA)

Asia where 71% of deposition comes from local sources. The maximum deposition reduction to the Arctic comes from the reductions in East Asian emissions because of its highest emissions.

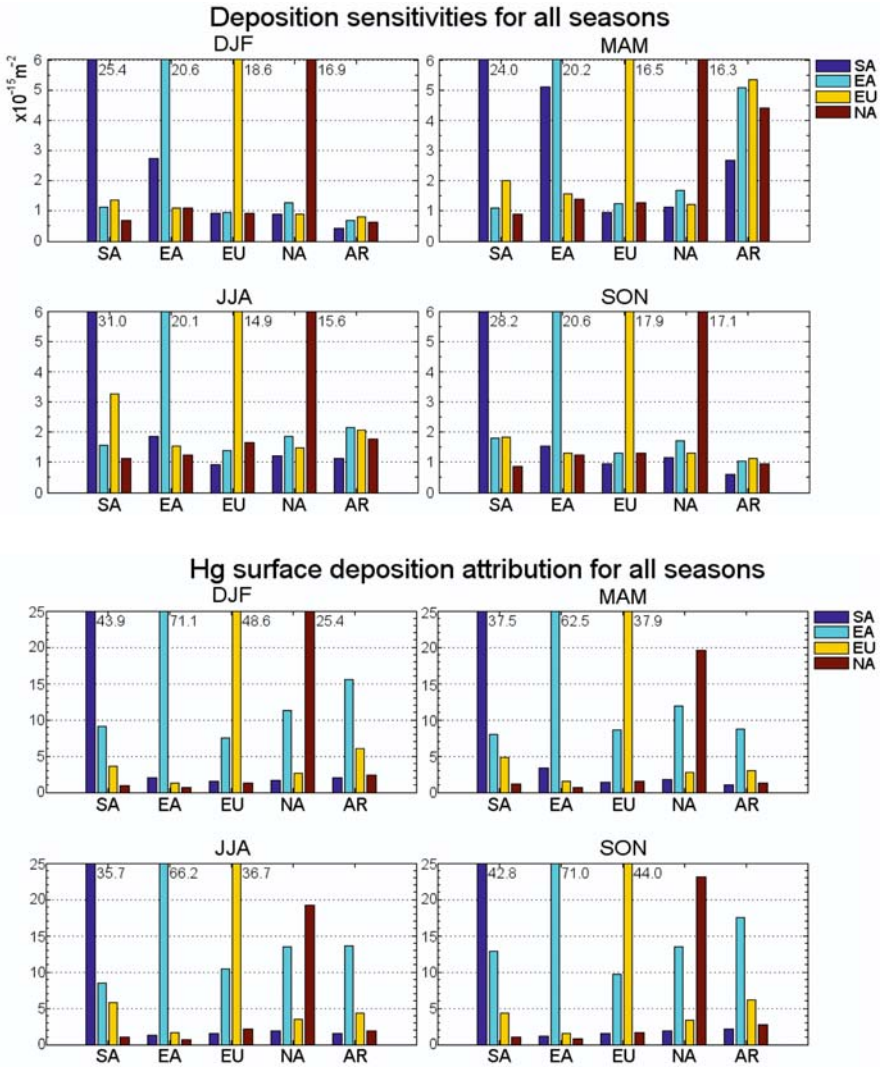

Figure 17.5 Mercury deposition sensitivities at receptor regions and the Arctic to unit emission reductions from the source regions defined as South Asia (SA), East Asia (EA), Europe and North Africa (EU) and North America (NA) (top). Percentage change in mercury deposition at receptor regions and the Arctic from 20% reduction in emissions at the source regions defined as above (the values are scaled to 100% reduction in the figure)

Numerous experimental and modelling studies have demonstrated the transpacific transport of air pollutant from East Asia to North America. The main mechanism for the rapid transport of Asian pollution is considered to be the lifting of boundary layer pollution into the free troposphere by mid-latitude cyclones. Once in the free troposphere over the western Pacific, Asian pollution can be transported undiluted to the northeastern Pacific in westerlies within 5 - 10 days. The subsiding air in anticyclones can bring the pollution to the lower levels affecting western North America and the Arctic. Convection and orographic lifting are also important mechanism in transporting Asian pollution. The transport across the Pacific is complex and usually involves several mid-latitude cyclones and associated warm conveyor belts. Springtime is found to be the most active period for episodic transport of Asian pollution to North America. East Asian mercury emissions are roughly half of the anthropogenic emissions globally.

The deposition contribution from East Asia to North America is estimated to be ~14% in this study. Jaffe et al., (2005) identified several Asian outflow of mercury at Hedo Station, Okinawa, Japan and the Mt. Bachelor Observatory in central Oregon, USA during spring 2004. They observed mean GEM concentrations of 2.04 ng m^{-3} at Hedo Station which is higher than the Northern Hemispheric background value of 1.8 ng m^{-3} due to the impact of Asian ouflow. They identified several long-range transport episodes at Mt. Bachelor. One large episode was observed around 25 April where the peak total Hg concentrations reached ~2.5 ng m^{-3} which is 0.7 ng m^{-3} above the background value. They found GEM/CO ratio at Mt. Bachelor to be very similar to the GEM/CO ratio found at Hedo Station. Using GEM/CO ratio and CO emissions, they estimated mercury emissions from Asia two times higher than the Asian mercury emissions estimates by Pacyna et al. (2006). In order to investigate the origin of high concentrations of mercury at Mt. Bachelor and the transport mechanism during the episode of April 25, 2004, we performed a series of GRAHM simulations at various resolutions. We found that the model simulated the observed episode best at resolution $0.25° \times 0.25°$ lat-long (Figure 17.6).

We performed simulations with all global emissions, only Asian anthropogenic emissions and other anthropogenic emissions. The top panel in the figure shows GEM mixing ratios at 500 hPa from all emissions on April 25, 2004. The bottom panel shows GEM mixing ratios at 500 hPa from only Asian emissions. Transpacific transport of mercury and significantly high concentrations of GEM along western coast of North America on April 25 are well simulated by the model. The model simulation with only Asian emissions reproduces the episodic transpacific transport of mercury from East Asia to North America and high concentrations of mercury around Oregon on April 25 suggesting East Asia to be the origin of this episode. Although, the depth of the peak in mercury concentrations at Mt. Bachelor is reproduced in all emissions simulation, it is underpredicted in only Asian emissions. Comparison of the two simulations suggests significant contribution of re-emissions and/or natural emissions in addition to the contribution from direct anthropogenic emissions from Asia.

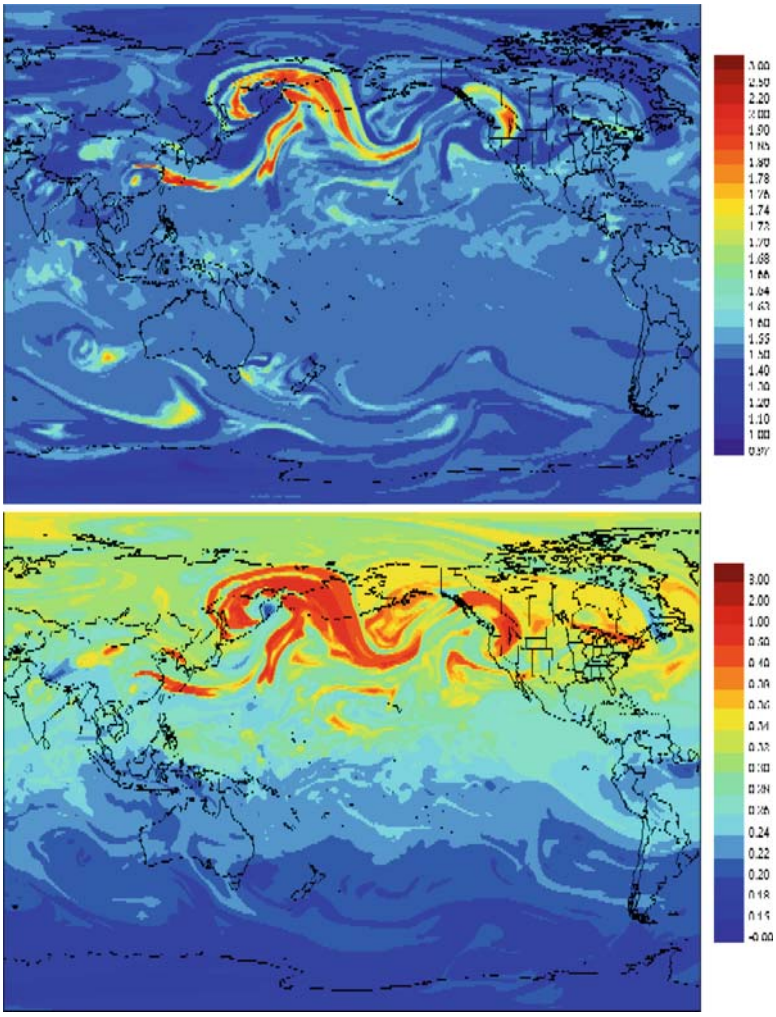

Figure 17.6 GRAHM air concentrations of mercury (*ng standard* m^{-3}) on 18 April 25, 2004 at 500 mb showing episode of Asian outflow of mercury reaching N. America which was observed at Mt. Bachelor in central Oregon. The top anthropogenic panel shows simulation from all emissions and the bottom panel shows simulation from anthropogenic Asian emissions

17.4 Uncertainties and Future Research

Deposition of mercury to a region from remote sources involves long range transport of GEM and its conversion to hygroscopic mercury species (RGM and Hg(p)). Current understanding of atmospheric chemistry and kinetics are based on limited laboratory and theoretical studies. Some of the reactions are not clearly defined and

reaction products are not well understood. Although, several gas phase oxidation pathways including O_3, OH and Br have been suggested for removal of GEM in the troposphere by the laboratory studies, their relative importance in establishing the observed tropospheric life time of GEM is not clear. Fast oxidation rates measured for some of these reactions suggest presence of significant reduction processes of mercury in the atmosphere which are yet to be identified. Comprehensive understanding of the mercury chemistry and adequate measurements of mercury species in free troposphere are required for improving the mercury chemical mechanism in the model. We have included the halogen mercury chemistry in the MBL and the Polar boundary layer which relies on halogen concentration estimates from observations. Model development will be continued to include representation of halogen liberation mechanism and halogen chemistry in the model. Accurate understanding and modelling of mercury exchange at the land/ocean/air interface is required to improve the characterization of long range transport of mercury for better attribution of sources of mercury in deposition. Presently, GRAHM includes dynamic exchange of mercury between snow and air, whereas land and ocean are assumed to have longer response time compared to the simulation period. We are investigating coupling of GRAHM with terrestrial and ocean models to improve the surface interactions in the model. The dry deposition of mercury to different surfaces and wet deposition over the oceans are not constrained by observations in the model due to the lack of such measurement data. Poor speciation of anthropogenic emissions is another source of uncertainty in attributing the emission sources to the deposition in the model.

References

Ariya, P., A. Dastoor, M. Amyot, W. Schroeder, L. Barrie, K. Anlauf, F. Raofie, A. Ryzhkov, D. Davignon, J. Lalonde, A. Steffen, 2004. Arctic: A sink for mercury. *Tellus*, 56B, 397–403.

Calvert, J.G., S.E. Lindberg, 2005. Mechanisms of mercury removal by O3 and OH in the atmosphere. *Atmospheric Environment*, 39, 3355–3367.

Dastoor, A.P., Y. Larocque, 2004. Global circulation of atmospheric mercury: A modeling study. *Atmospheric Environment*, 38, 147–161.

Dastoor, A.P., D. Davignon, N. Theys, M. Roozendael, A. Steffen and P.A. Ariya, 2008. Modeling Dynamic Exchange of Gaseous Elemental Mercury at Polar Sunrise. Environmental Science and Technology (in press).

Donohoue, D.L., D. Bauer, B. Cossairt, and A. J. Hynes, 2006. Temperature and pressure dependent rate coefficients for the reaction of Hg with Br and the reaction of Br with Br: A pulsed laser photolysis-pulsed laser induced fluorescence study. *Journal Physical Chemistry A*, 110, 6623–6632.

Hall, B., 1995. The gas phase oxidation of elemental mercury by ozone. *Water, Air, and Soil Pollution*, 80, 301–315.

Hammerschmidt CR, W.F. Fitzgerald, 2004. Geochemical controls on the production and distribution of methylmercury in near-shore marine sediments. *Environmental Science and Technology*, 38, 1487–1495.

Horowitz, L. W., S. Walters, D. L. Mauzerall, L. K. Emmons, P.J. Rasch, C. Granier, X. Tie, J.-F. Lamarque, M.G. Schultz, G.P. Brasseur, 2003. A global simulation of tropospheric ozone and

related tracers : Description and evaluation of MOZART, version 2, *Journal of Geophysical Research* , 108(D24), 4784, doic 10.1029/2002JD002853.

Jaffe, D., E. Prestbo, P. Swartzendruber, P. Weiss-Penzias, S. Kato, A. Takami, S. Hatakeyama and Y. Kajii, 2005, Export of atmospheric mercury from Asia. *Atmospheric Environment*, 39, 3029–3038.

Kirk, J.L., V.L. St. Louis, M.J. Sharp, 2006. Rapid reduction and reemission of mercury deposited into snowpacks during atmospheric mercury depletion events at Churchill, Manitoba, Canada. *Environmental Science and Technology*, 40, 7590–7596.

Laurier, F. J. G., R. P. Mason, L. Whalin, S. Kato, 2003. Reactive gaseous mercury formation in the North Pacific Ocean's marine boundary layer: A potential role of halogen chemistry. *Journal of Geophysical Research*, 108, D17, art # 4529.

Lin, C.-J., P. Pongprueksa, S.E. Lindberg, S.O. Pehkonen, D. Byun, C. Jang, 2006. Scientific uncertainties in atmospheric mercury models I: Model science evaluation. *Atmospheric Environment*, 40, 2911–2928.

Mason, R. P., G.-R Sheu, 2002. The role of the ocean in the global mercury cycle. *Global Biogeo. Cycles*, 16, art. # 1093.

Outridge, P.M., R.W. Macdonald, F. Wang, G.A. Stern and A.P. Dastoor, 2008. A mass balance inventory of mercury in the Arctic Ocean. *Environmental Chemistry*, 5, 89–111. doi:10.1071/EN08002.

Pacyna, E. G., Pacyna, J. M., Steenhuisen, F., Wilson, S., 2006. Global anthropogenic mercury emission inventory for 2000. *Atmospheric Environment*, 40, 4048–4063.

Poulain, A.J., J.D. Lalonde, M. Amyot, J.A. Shead, F. Raofie, P.A. Ariya, 2004. Redox transformations of mercury in an Arctic snowpack at springtime. *Atmospheric Environment*, 38, 6763–6774.

Steffen, A., Douglas, T., Amyot, M., Ariya, P., Aspmo, K., Berg, T., Bottenheim, J., Brooks, S., Cobbett, F., Dastoor, A., Dommergue, A., Ebinghaus, R., Ferrari, C., Gardfeldt, K., Goodsite, M.E., Lean, D., Poulain, A., Scherz, C., Skov, H.,Sommar, J., Temme, C., 2008. A synthesis of atmospheric mercury depletion event chemistry in the atmosphere and snow. *Atmospheric Chemistry and Physics*, 8, 1445–1482.